Nanostructures

DOI: 10.1002/anie.200704909

Transparent Carbon Films as Electrodes in Organic Solar Cells**

Xuan Wang, Linjie Zhi, Nok Tsao, Željko Tomović, Jiaoli Li, and Klaus Müllen**

Indium tin oxide (ITO) has been widely used as an electrode material in optoelectronic devices because of its high conductivity, good transmittance, and suitable work function. The use of ITO, however, appears to be increasingly problematic because of both the limited availability of the element indium on earth and the intrinsic chemical and electrical drawbacks of ITO.[1] Several candidates have been reported to replace ITO, such as other transparent conducting oxides (TCOs),[2] conducting polymer films,[3] as well as carbon nanotube (CNT) films,[4] for the fabrication of devices such as organic light-emitting diodes and solar cells. The limited thermal and chemical stability (polymer films and TCOs) and relatively high surface roughness (CNT films) are disadvantages of these films. An alternative and attractive option would be the use of thin graphene-based films, since recent studies have shown that graphene sheets, generally produced by a top-down exfoliation of graphites, have remarkable electronic properties.[5] Herein we present a new bottom-up chemical approach towards the synthesis of transparent graphene-constructed films (TGFs) as electrodes. This has been achieved by the thermal reaction of synthetic nanographene molecules of giant polycyclic aromatic hydrocarbons (PAHs) which are cross-linked with each other and further fused into larger graphene sheets. The fabrication and characterization of the TGFs and their successful use as hole-collecting electrodes in organic solar cells are described.

Extremely large PAHs, such as nanographene molecules, are suitable units for the bottom-up construction of graphene sheets by thermal fusion at high temperatures by stepwise heat treatment.[6] Flexible alkyl side chains on the periphery are necessary to promote the solubility of PAHs and thus enable simple solution processing.[7] Herein, one discotic liquid crystal,[7a] a superphenalene derivative **1**, which has both a large aromatic core and good solubility (Figure 1a), was taken as a typical example. The solution was spin-coated onto substrates and then heated at 1100 °C in an Ar atmosphere. The resulting conductive graphene-constructed films were sufficiently thin to be transparent over the relevant range of wavelengths.

The transparency of the TGFs on quartz could be tuned by controlling the film thickness by varying the solution concentration. The transmission contrast of the hollow letters "M", "P", "I", and "P" in the middle of the TGFs and the text lying behind these films highlighted the increase in transmittance

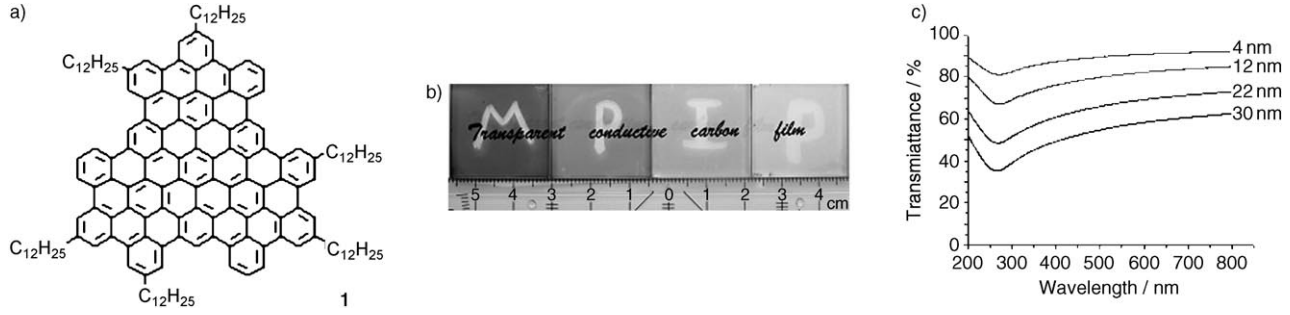

1

Figure 1. a) Molecular structure of **1**, the hexadodecyl-substituted superphenalene C96-C_{12}; b) 30, 22, 12, and 4 nm-thick TGFs on quartz (2.5 × 2.5 cm^2) with "M", "P", "I", and "P" letters inside, erased from the film before heat treatment; c) transmission spectrum of the TGFs with different thicknesses.

with a decrease of the film thickness (Figure 1b). TGFs with thicknesses of 30, 22, 12, and 4 nm have transmittances of 55, 66, 80, and 90%, respectively, at a wavelength of 500 nm (Figure 1c). In addition, for a given film thickness, the transmittance was dependent upon the wavelength, with a minimum value at about 260 nm, which implies the TGFs have a graphitic structure.[8]

The electrical characteristics of the as-prepared 30-nm-thick TGFs were evaluated by a four-point probe measurement, which showed a sheet resistance of 1.6 kOhm $square^{-1}$ and a conductivity of 206 S cm^{-1}. A small decrease in the film conductivity was observed as the film thickness decreased (Figure 2a). The structure of the TGFs, as characterized by high-resolution transmission electron microscopy (HRTEM; Figure 2c) and Raman spectroscopy (see the Supporting

[*] Dr. X. Wang, Dr. L. Zhi, N. Tsao, Dr. Ž. Tomović,[+] Dr. J. Li, Prof. Dr. K. Müllen
Max-Planck Institute for Polymer Research
Ackermannweg 10, 55128 Mainz (Germany)
Fax: (+49) 6131-379-350
E-mail: zhi@mpip-mainz.mpg.de
muellen@mpip-mainz.mpg.de

[+] Present address:
Elastogran, BASF group, Global PU Specialties Research
Elastogranstrasse 60, 49448 Lemförde (Germany)

[**] This work was financially supported by the Deutsche Forschungsgemeinschaft (SFB 625) and the Max Planck Society through the program ENERCHEM. We thank Dr. C. G. Clark, Jr. for his help in the preparation of the manuscript.

Supporting information for this article is available on the WWW under http://www.angewandte.org or from the author.

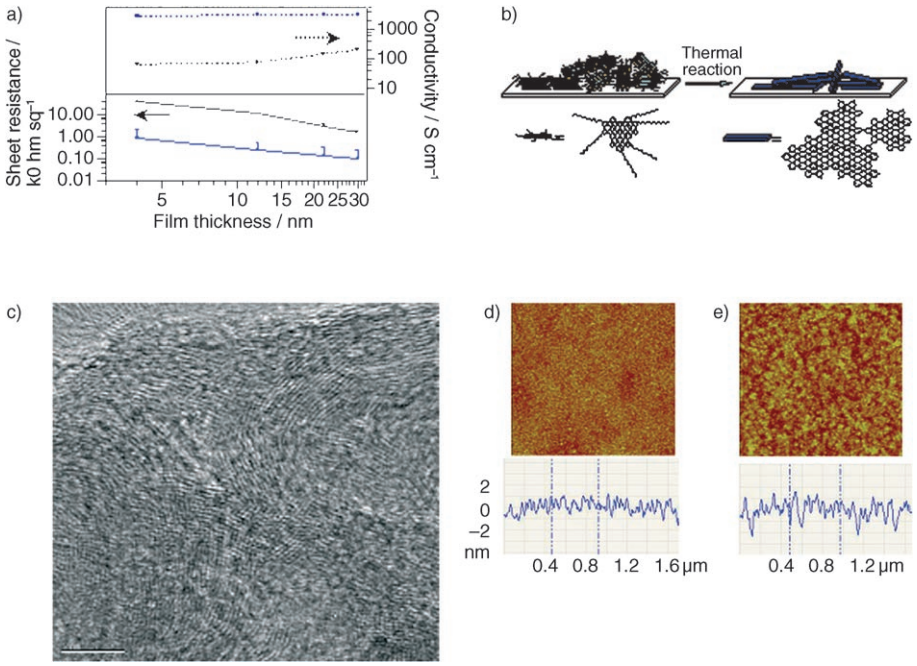

Figure 2. a) Sheet resistance (solid curves with half error bars in the plus direction) and corresponding average conductivity (short dashed curves) of the TGFs as a function of the film thickness, with the plot in the log-log scale. Black and blue curves denote the TGFs produced on quartz and SiO_2/Si, respectively. b) Illustration of the mechanism of the intermolecular condensation of nanographene **1** into graphitic networks. c) A representative HRTEM image of a TGF (scale bar: 5 nm). d),e) AFM height images ($2\times2\ \mu m^2$) of 4- and 30-nm-thick TGF surfaces, respectively (color scale: black to bright yellow, 10 nm). Each image is accompanied with a cross-sectional plot which has the same verticle scale.

Information), clearly consisted of ordered, tightly packed graphene layers, which were formed by the fusion of nanographenes by the programmed heating procedure (see the Supporting Information). This process stabilized the orientation of the nanographene molecules on substrates in short order and induced intermolecular condensation to form graphitic networks (Figure 2b) at higher temperatures. It is thus believed that the microstructure and conductivity of the TGFs depend on the molecular organization, which is related to the interaction between the substrates and the molecules[9] during heat treatment. The conductivity of the TGFs was greatly enhanced to approximately 3000 $S\,cm^{-1}$ by using SiO_2/Si as the substrate (Figure 2c), which could be due to an improvement in the organization of nanographene **1** on SiO_2/Si during the heat treatment (see the Supporting Information).

Smooth surfaces as well as high mechanical and stable chemical properties are key requirements for electrodes used in optoelectronic devices. Compared with the relatively rough surface and chemical instability of ITO, an ultrasmooth surface was characteristic of the TGFs, as illustrated by atomic force microscopy (AFM), which showed the absence of large aggregates, pinholes, and cracks (Figure 2d,e). The average surface roughness (R_a) of the TGFs with thicknesses of 4, 12, and 30 nm over a $2\times2\ \mu m^2$ area was 0.4, 0.5, and 0.7 nm, respectively. At the same time, the TGFs remained intact after a prolonged bath ultrasonication in common organic solvents and passed the laboratory Scotch-tape test,[10] thus revealing the strong adhesion of TGFs to the substrates.

After immersing the TGF/quartz into piranha solution (a mixture of concentrated sulfuric acid and H_2O_2) for 48 h, the TGF still exhibited good conductivity, comparable to that of the original film.

To demonstrate how the TGFs performed as anodes, organic solar cells were fabricated using a blend of poly(3-hexyl)thiophene (P3HT) and phenyl-C_{61}-butyric acid methyl ester (PCBM; Figure 3a,b). The photoactive composite layer was sandwiched between TGF/quartz and an Ag electrode. The TGF on quartz had a sheet resistance of 18 $kOhm\,square^{-1}$ and a transmittance of 85% at 500 nm.

The devices were illuminated with monochromatic light and the highest external quantum efficiency (EQE) of around 43% was achieved at a wavelength of 520 nm (Figure 3c). This efficiency is comparable to the highest EQE value of 47% for a reference device fabricated under similar conditions but with ITO/glass as the anode.

The current–voltage (*I–V*) characteristics of the device (Figure 3d) showed a distinct diode behavior

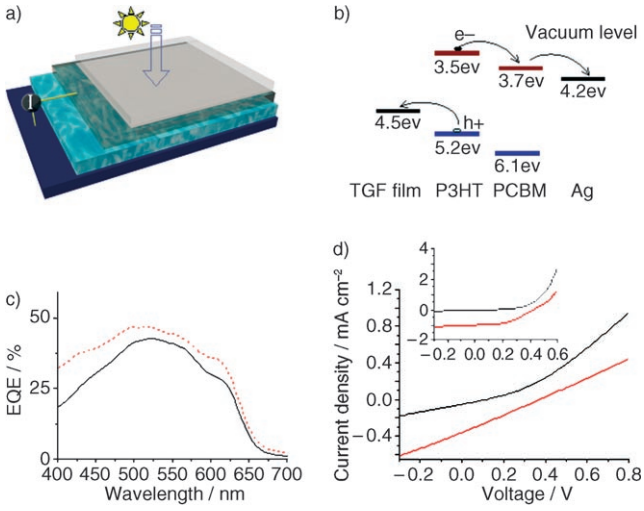

Figure 3. a) Illustration of the solar cell; the four layers from bottom to top are Ag, a blend of P3HT and PCBM, TGF, and quartz, respectively. b) A schematic representation of charge transfer and transport as an energy level diagram; the work function has not been measured for TGFs, but it was presumed to be 4.5 eV.[11] c) EQE of a TGF-based cell (solid black curve) and an ITO-based cell (red dashed curve). d) *I–V* curve of a TGF-based cell (center) and an ITO-based cell (inset) illuminated under simulated solar light (red curve) and with monochromatic light of wavelength 510 nm (black curve). The calibrated light intensity of the simulated solar light is 167 $W\,m^{-2}$ for ITO and 119 $W\,m^{-2}$ for TGF as anode.

under monochromatic light with a wavelength of 510 nm. The short-circuit photocurrent density (I_{sc}), open-circuit voltage (V_{oc}), calculated filling factor (FF), and overall power conversion efficiency (η) are listed in Table 1. The similar

Table 1: Performance of the solar cells based on TGF and ITO as anodes.

Light	Anode	I_{sc} [mA cm^2]	V_{oc} [V]	FF	η
monochromic light of 510 nm	ITO	0.04	0.14	0.3	1.5
	TGF	0.052	0.13	0.23	1.53
simulated solar light	ITO	1.0	0.41	0.48	1.17
	TGF	0.36	0.38	0.25	0.29

power conversion efficiency indicates that the TGF-based cell is as good as the ITO-based cell under low intensity monochromatic illumination. Furthermore, when illuminated with simulated solar light, the cell gave a comparable V_{oc} value to that of the ITO-based cell, which suggests an appropriate work function of the TGFs as the anode.[12] The relatively lower values of I_{sc}, FF, and EQE in comparison with that of the reference cell are likely due to the relatively higher sheet resistance of the TGFs used, which could be improved.

The concept of using TGFs as window electrodes in solar cells emerges as a very practicable option for future devices, although the performance of the solar cell shown here is in an un-optimized state. The outstanding thermal and chemical stability as well as the ultrasmooth surface make TGFs suitable not only for organic solar cells but particularly for hybrid dye-sensitized solar cells.[13] Furthermore, simple processing enables inexpensive and large-scale industrial manufacturing. Besides spectroelectrochemical applications,[14] such TGFs have great potential in the fabrication of flat-panel displays, organic light-emitting diodes (OLEDs), and other modern optoelectronic devices.

Experimental Section

Film preparation: Compound C96-C_{12}[7a] was dissolved in chloroform at a concentration of 1.25 to 7.5 mg mL^{-1} and the solution was spin-coated onto the substrates. The substrate was first heated at 400 °C for 4 h and then at 1100 °C for 30 min with a rate of temperature increase of 2 °C min^{-1} under Ar.

Device fabrication and testing: The photoactive composite layer was spin-coated from an 18 mg mL^{-1} solution of P3HT and PCBM (weight ratio 1:0.8) in chlorobenzene onto a TGF/quartz substrate, which was pretreated with acetone and isopropanol in an ultrasonic bath. A cathode was formed by subsequently evaporating a 100-nm-thick layer of silver onto the surface. The device was then annealed at 140 °C for 30 min. The testing conditions are described elsewhere.[15] For comparison, the ITO-based device was prepared and tested under relatively simple conditions without using a poly(3,4-ethylene dioxythiophene)/poly(styrene sulfonate) (PEDOT/PSS) buffer layer or other techniques developed in the literature, since the techniques developed for ITO-based devices might not necessarily meet the needs of TGF-based devices. Further improvement of the fabrication procedures as well as the performance of the cells is ongoing.

Received: October 23, 2007
Revised: January 22, 2008
Published online: March 10, 2008

Keywords: electrochemistry · graphene · nanostructures · solar cells

[1] a) A. R. Schlatmann, D. W. Floet, A. Hillberer, F. Garten, P. J. M. Smulders, T. M. Klapwijk, G. Hadziioannou, *Appl. Phys. Lett.* **1996**, *69*, 1764 – 1766; b) J. C. Scott, J. H. Kaufman, P. J. Brock, R. Dipietro, J. Salem, J. A. Goitia, *J. Appl. Phys.* **1996**, *79*, 2745 – 2751.

[2] J. Cui, A. C. Wang, N. L. Edleman, J. Ni, P. Lee, N. R. Armstrong, T. J. Marks, *Adv. Mater.* **2001**, *13*, 1476 – 1480.

[3] a) F. L. Zhang, M. Johansson, M. R. Andersson, J. C. Hummelen, O. Inganäs, *Adv. Mater.* **2002**, *14*, 662 – 665; b) W. H. Kim, A. J. Mäkinen, N. Nikolov, R. Shashidhar, H. Kim, Z. H. Kafafi, *Appl. Phys. Lett.* **2002**, *80*, 3844 – 3846; c) G. Gustafsson, Y. Cao, G. M. Treacy, F. Klavetter, N. Colaneri, A. J. Heeger, *Nature* **1992**, *357*, 477 – 479; d) Y. Yang, A. J. Heeger, *Appl. Phys. Lett.* **1994**, *64*, 1245 – 1247.

[4] a) S. Stankovich, D. A. Dikin, G. H. B. Dommett, K. M. Kohlhaas, E. J. Zimney, E. A. Stach, R. D. Piner, S. T. Nguyen, R. S. Ruoff, *Nature* **2006**, *442*, 282 – 286; b) A. K. Geim, K. S. Novoselov, *Nat. Mater.* **2007**, *6*, 183 – 191; c) K. S. Novoselov, A. K. Geim, S. V. Morozov, D. Jiang, Y. Zhang, S. V. Dubonos, I. V. Grigorieva, A. A. Firsov, *Science* **2004**, *306*, 666 – 669.

[5] a) M. Zhang, S. L. Fang, A. A. Zakhidov, S. B. Lee, A. E. Aliev, C. D. Williams, K. R. Atkinson, R. H. Baughman, *Science* **2005**, *309*, 1215 – 1219; b) M. E. Itkis, F. Borondics, A. Yu, R. C. Haddon, *Science* **2006**, *312*, 413 – 416; c) Z. C. Wu et al., *Science* **2004**, *305*, 1273 – 1276, see the Supporting Information; d) K. Lee, Z. Wu, Z. Chen, F. Ren, S. J. Pearton, A. G. Rinzler, *Nano Lett.* **2004**, *4*, 911 – 914; e) A. D. Pasquier, H. E. Unalan, A. Kanwal, S. Miller, M. Chhowalla, *Appl. Phys. Lett.* **2005**, *87*, 203511 – 203513; f) J. F. Li, L. B. Hu, L. Wang, Y. X. Zhou, G. Grüner, T. J. Marks, *Nano Lett.* **2006**, *6*, 2472 – 2477.

[6] a) L. J. Zhi, J. S. Wu, J. X. Li, U. Kolb, K. Müllen, *Angew. Chem.* **2005**, *117*, 2158 – 2161; *Angew. Chem. Int. Ed.* **2005**, *44*, 2120 – 2123; b) L. Gherghel, C. Kubel, G. Lieser, H. J. Rader, K. Müllen, *J. Am. Chem. Soc.* **2002**, *124*, 13130 – 13138.

[7] a) Ž. Tomović, M. D. Watson, K. Müllen, *Angew. Chem.* **2004**, *116*, 773 – 777; *Angew. Chem. Int. Ed.* **2004**, *43*, 755 – 758; b) M. D. Watson, A. Fechtenkotter, K. Müllen, *Chem. Rev.* **2001**, *101*, 1267 – 1300; c) L. Schmidt-Mende, A. Fechtenkötter, K. Müllen, E. Moons, R. H. Friend, J. D. MacKenzie, *Science* **2001**, *293*, 1119 – 1122.

[8] M. Chhowalla, H. Wang, N. Sano, K. B. K. Teo, S. B. Lee, G. A. J. Amaratunga, *Phys. Rev. Lett.* **2003**, *90*, 155504 – 155507.

[9] M. Keil, et al., *J. Phys. Chem. B.* **2000**, *104*, 3967 – 3975, see the Supporting Information.

[10] A. G. Rinzler, et al., *Appl. Phys. A* **1998**, *67*, 29 – 37, see the Supporting Information.

[11] J. W. G. Wildoeer, L. C. Venema, A. G. Rinzler, R. E. Smalley, C. Dekker, *Nature* **1998**, *391*, 59 – 62.

[12] H. Frohne, S. E. Shaheen, C. J. Brabec, D. C. Müller, N. S. Sariciftci, K. Meerholz, *ChemPhysChem* **2002**, *3*, 795 – 799.

[13] U. Bach, D. Lupo, P. Comte, J. E. Moser, F. Weissörtel, J. Salbeck, H. Spreitzer, M. Grätzel, *Nature* **1998**, *395*, 583 – 585.

[14] a) J. S. Mattson, C. A. Smith, *Anal. Chem.* **1975**, *47*, 1122 – 1125; b) T. P. DeAngells, R. W. Hurst, A. M. Yacynych, H. B. Mark, W. R. Helneman, J. S. Mattson, *Anal. Chem.* **1977**, *49*, 1395 – 1398; c) S. Donner, H. W. Li, E. S. Yeung, M. D. Porter, *Anal. Chem.* **2006**, *78*, 2816 – 2822.

[15] J. L. Li, F. Dierschke, J. S. Wu, A. C. Grimsdale, K. Müllen, *J. Mater. Chem.* **2006**, *16*, 96 – 100.

